# Fully self-consistent nova explosion models reproducing light curves of KT Eri, V339 Del, V597 Pup, and SMC NOVA 2016-10a

Mariko Kato<sup>©</sup>, Izumi Hachisu<sup>©</sup>, and Hideyuki Saio<sup>3</sup>

Department of Astronomy, Keio University, Hiyoshi, Kouhoku-ku, Yokohama 223-8521, Japan
 Department of Earth Science and Astronomy, College of Arts and Sciences, The University of Tokyo, 3-8-1 Komaba, Meguro-ku, Tokyo 153-8902, Japan

# ABSTRACT

The rising phase toward the optical maximum of a classical nova is one of the last frontiers of nova study. Constructing free-free emission model light curves based on our fully self-consistent nova explosion models, we present several theoretical light curves of classical novae and compare them with the four novae having the observed rising phase toward the optical maximum. Our 1.25  $M_{\odot}$  white dwarf (WD) models show excellent agreements with the light curves of KT Eri, V339 Del, and V597 Pup while our 1.35  $M_{\odot}$  WD models are consistent with the light curves of SMC NOVA 2016-10a. These agreements indicate that the light curves toward the optical maximum of these novae are dominated by free-free emission, rather than by photospheric emission. Our results justify the previously obtained WD masses and distance moduli for these novae, and shows that the post-maximum evolution can be well approximated with the evolution sequences of steady-state envelope solutions.

Keywords: novae, cataclysmic variables — stars: individual (KT Eri, V339 Del, V597 Pup, SMCN 2016-10a) — stars: winds

# 1. INTRODUCTION

A nova is a thermonuclear runaway event that occurs on an accreting white dwarf (WD) in a binary (e.g., K. Nariai et al. 1980; I. Jr., Iben 1982; D. Prialnik & A. Kovetz 1995; E. M. Sion et al. 1979; W. N. Sparks et al. 1978; A. Tajitsu et al. 2015). After the thermonuclear runaway sets in, the WD becomes bright and its surface temperature increases to  $T_{\rm ph} \sim 10^6$  K and emits supersoft X-rays in a short time. This very early phase phenomenon is called the X-ray flash (O. König et al. 2022; M. Kato et al. 2022b). The WD envelope expands and the photospheric temperature decreases. Strong winds emerge from the WD photosphere when the photospheric temperature decreases to  $T_{\rm ph} \sim 10^{5.4}~{\rm K}$  (e.g., M. Kato & I. Hachisu 1994). Then the X-ray flash phase ends. Winds are accelerated deep inside the photosphere (M. Friedjung 1966; C. L. N. Ruggles & G. T. Bath 1979) so that they are called the optically thick winds. Winds become optically thin outside the WD photosphere. The WD photosphere further expands toward optical maximum and the nova becomes brighter in the optical band owing to free-free emission from the optically thin ejecta (e.g., D. Ennis et al. 1977; J. S. Gallagher & E. P. Ney 1976; I. Hachisu & M. Kato 2006, 2025b).

At the optical maximum, the WD photosphere reaches maximum (radius) and the wind mass-loss rate also reaches maximum. After the maximum expansion of the photosphere, the WD envelope (interior to the photosphere) quickly loses its mass mainly due to wind mass loss. The mass loss rate becomes smaller and thus, free-free emission becomes fainter. As most of the envelope mass is blown in the wind, the WD photosphere shrinks and the photospheric temperature increases. Then the optically thick winds finally end and the nova enters the supersoft X-ray source (SSS) phase (J. Krautter et al. 1996; G. J. Schwarz et al. 2011; M. Henze et al. 2011, 2015, 2018; K. L. Page et al. 2022). Finally, nuclear burning ends and the WD becomes faint.

Nova light curves have been difficult to calculate with Henyey-type evolution codes especially after the opacity

 $<sup>^3</sup> A stronomical\ Institute,\ Graduate\ School\ of\ Science,\ Tohoku\ University,\ Sendai\ 980-8578,\ Japan$ 

tables are revised (C.A. Iglesias & F. J. Rogers 1993; C.A. Iglesias & F.J. Rogers 1996; M. J. Seaton et al. 1994) that shows a large Fe peak at around  $\log T$  (K) = 5.2 which accelerates envelope expansion. merical difficulty appears when the diffusive luminosity approaches the local Eddington luminosity in the extended nova envelope. Many authors adopt some technique to continue evolution calculation, i.e., to skip the extended stage assuming a large massloss (e.g., P.A. Denissenkov et al. 2013; X. Ma et al. 2013; C. Wu et al. 2017; H.-L. Chen et al. 2019) or including convection in the supersonic region (e.g., K. J. Shen & E. Quataert 2022). If we adopt such methods, we can hardly calculate accurate optical light curves because the photospheric temperature becomes  $\sim 10^4$  K or less at the optical peak, much lower than the Fe opacity peak ( $\log T$  (K)  $\approx 5.2$ ) (see M. Kato et al. 2017a, for a review and comparison among various approximations of the numerical methods).

Thus, actually no accurate theoretical light curves have ever been presented except Kato's group. A rare exception is Y. Hillman et al. (2014) who presented theoretical light curves of nova outbursts based on the calculation by D. Prialnik & A. Kovetz (1995). However, their V light curves show a flat-peak followed by a sudden drop as a rectangular shape, which are very different from gradual declines in observed nova light curves. The reason is partly a small number of mass grids (see Figure 9 in Y. Hillman et al. 2016) and inadequate surface boundary condition as pointed out in Figure 6 of M. Kato et al. (2017a).

M. Kato et al. (2022a) succeeded, for the first time, in calculating one cycle of nova evolution including extended phase of the envelope. They determined wind mass loss rates which are consistent with the continuum-radiation driven wind by the Fe peak. Using this method, M. Kato et al. (2025) calculated the V light curve of a 1.35  $M_{\odot}$  WD and reproduced the V1674 Her observation including the very early rising phase (see also I. Hachisu & M. Kato 2025b, for an extremely early phase).

The optical rising phase toward the optical peak of a nova outburst has been poorly studied partly because of lack of theoretical models as well as the paucity of observational data. We have calculated several nova light curves of 1.25  $M_{\odot}$  and 1.35  $M_{\odot}$  WDs, which enable us quantitative comparison with observed nova outburst data around the optical peak. Our aim of this paper is to compare the observed data with our theoretical light curves and clarify its physics.

This paper is organized as follows. Section 2 explains our numerical method and presents our optical light curves based on our free-free emission model. Section 3 compares our model light curves with the four classical novae, KT Eri, V339 Del, V597 Pup, and SMC Nova 2016-10a. Our discussion and conclusions follow in Sections 4 and 5.

# 2. MODEL LIGHT CURVES OF NOVAE

# 2.1. Numerical Method

We have calculated nova outburst cycles for 1.25  $M_{\odot}$ and 1.35  $M_{\odot}$  WDs with several mass accretion rates. We assume spherical symmetry and solve interior structure from the center of the WD up to the photosphere. We do not calculate outside the WD photosphere, even if winds extend over the WD photosphere. We use a Henyeytype stellar evolution code consistently connected with steady-state wind solutions in each time-step to determine the wind mass-loss rate. The typical number of the mass zones is slightly less than or about 1000 for the WD interior the region of which we solve with the Henyey code, and several thousands mass zones for the wind solutions which are solved with the steady-state hydrodynamic code (M. Kato & I. Hachisu 1994). The time-steps, which depend on the mass-accretion rate, are taken to be 0.01-0.05 s during the thermonuclear runaway phase, 100-10,000 s near the optical peak, and a few tens of years for the quiescent phase. This method requires complicated and time-consuming human iteration procedure to fit the interior with the exterior envelope solution in each time step, but enable us to calculate one full cycle nova evolution including extended envelope phase around the optical peak.

For the initial WD model we have adopted a steady-state equilibrium model (M. Kato et al. 2014), in which the heating by the mass accretion and nuclear energy generation is balanced with the cooling by radiative diffusion and neutrino emission. Starting from the steady-state WD model, the flash properties reach a limit cycle before 5th flash cycle, which indicates that the interior structure of our initial model is already a good approximation to the structure reached after many flashes. The method of our numerical calculation is described in M. Kato et al. (2022a, 2024, 2025).

We have assumed a solar composition for accreting matter (X=0.7, Y=0.28, and Z=0.02). The composition of the CO core is composed of 48% of  $^{12}$ C, 50% of  $^{16}$ O, and 2% of  $^{20}$ Ne by mass. This ratio of C, O, and Ne does not affect our results of a nova outburst. We used the OPAL opacity tables (C.A. Iglesias & F.J. Rogers 1996).

Model	$M_{ m WD}$	$\dot{M}_{ m acc}$	C mix	$\log T_{ m WD}$	$t_{ m rec}$	$L_{ m nuc}^{ m max}$	$M_{ m ig}$	$\log T^{\max}$	$R_{ m ph}$	$-\dot{M}_{ m wind}^{ m max}$
	$(M_{\odot})$	$(M_{\odot}~{ m yr}^{-1})$		(K)	(yr)	$(10^9 L_{\odot})$	$(10^{-6} M_{\odot})$	(K)	$(R_{\odot})$	$(10^{-5} M_{\odot} \text{ yr}^{-1})$
M125ac5E-11	1.25	$5 \times 10^{-11}$	0.1	7.44	120,000	27.0	6.1	8.27	82	26
M125ac1E-10	1.25	$1 \times 10^{-10}$	0.1	7.49	51,000	18.0	5.4	8.26	63	22
M125ac5E-10	1.25	$5 \times 10^{-10}$	0.1	7.58	8,100	9.3	4.3	8.24	42	17
M125ac1E-9	1.25	$1 \times 10^{-9}$	0.1	7.63	4,000	7.0	4.2	8.23	33	14
M125ac5E-9	1.25	$5 \times 10^{-9}$	0.1	7.74	520	1.6	2.8	8.19	16	8.3
M135ac1E-11	1.35	$1 \times 10^{-11}$	0.1	7.39	160,000	31	1.6	8.33	21	12
M135ac5E-10	1.35	$5 \times 10^{-10}$	0.1	7.61	1,900	5.8	1.0	8.28	14	8.8
M135ac5E-9	1.35	$5 \times 10^{-9}$	0.1	7.79	120	1.2	0.70	8.24	3.2	2.3

Table 1. Model Properties $^a$ 

Many classical novae show heavy element enrichment in ejecta (e.g., K. M. Vanlandingham et al. 1996, 1997; R. D. Gehrz et al. 1998; I. Hachisu & M. Kato 2006; G. J. Schwarz et al. 2007; K. V. Sokolovsky et al. 2023). To mimic such a heavy element enrichment, we have increased carbon mass fraction in the hydrogen-rich envelope by 0.1 and decreased helium mass fraction by the same amount at the beginning of thermonuclear runaway (S. Starrfield et al. 2020; M. Kato et al. 2024). The amount of carbon enrichment does not affect the results because the energy generation at ignition,  $L_{\rm nuc}^{\rm max}$ , is unchanged between the carbon mixtures of 0.1 and 0.2 (M. Kato et al. 2022c).

The model parameters and characteristic physical values are listed in Table 1. From left to right, model name, the WD mass, mass accretion rate in quiescent phase, assumed carbon enhancement in the hydrogen-rich envelope, temperature at the WD center, recurrence period of nova outbursts, maximum nuclear burning energy generation rate, ignition mass, i.e., mass of the hydrogen-rich envelope at the onset of thermonuclear runaway, the maximum temperature at hydrogen burning, photospheric radius at the maximum expansion, i.e., the WD radius at the optical peak, and the maximum mass-loss rate which is reached at the maximum expansion of the photosphere.

The basic properties of one cycle of a nova outburst, internal structures, optical and SSS light curves are already described in M. Kato et al. (2025) for models M135ac1E-11 and M135ac5E-10. The data of model M135ac5E-9 are partly reported in M. Kato et al. (2022b) only for the X-ray flash phase. The 1.25  $M_{\odot}$  WD models show essentially the same properties as those of the 1.35  $M_{\odot}$  WD models. Thus, in the present paper we concentrate on the early outburst phase, that

is, the optical rising phase, optical peak, and early decay phase.

# 2.2. Optical Light Curve

Assuming that the V band luminosity is dominated by free-free emission (e.g., D. Ennis et al. 1977; J. S. Gallagher & E. P. Ney 1976), we have calculated optical V light curves of each model. In the present paper, we do not include the contribution of the WD photosphere (blackbody assumption) because it is much fainter than that of free-free emission (see Discussion Section 4.1). The V band luminosity of free-free emission from optically thin plasma outside the WD photosphere can be simplified as (I. Hachisu & M. Kato 2006; I. Hachisu et al. 2020)

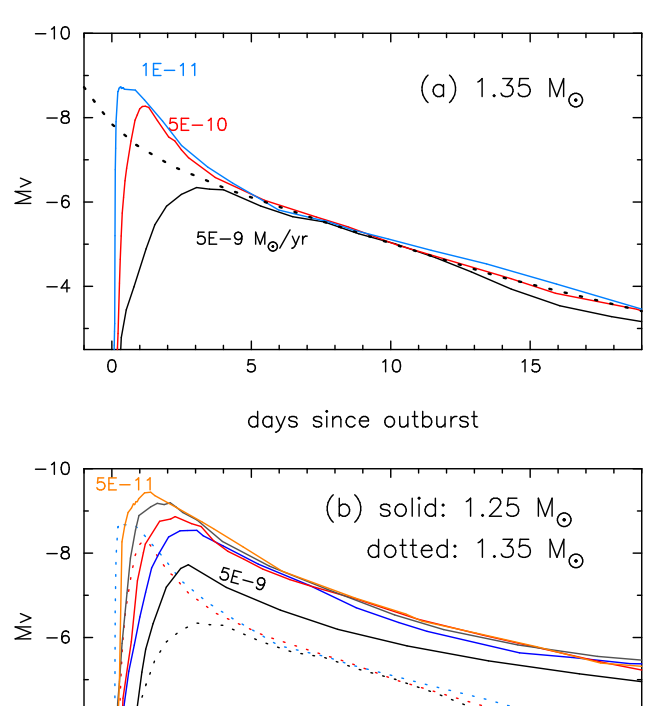
$$L_{V,\text{ff,wind}} = A_{\text{ff}} \frac{\dot{M}_{\text{wind}}^2}{v_{\text{ph}}^2 R_{\text{ph}}},\tag{1}$$

where  $\dot{M}_{\rm wind}$  is the wind mass loss rate,  $v_{\rm ph}$  the wind velocity at the WD photosphere, and  $R_{\rm ph}$  the photospheric radius of the WD. The coefficient  $A_{\rm ff}$  depends on the WD mass and chemical composition of the envelope. We have already determined the coefficient  $A_{\rm ff}$  by novae with known distances (I. Hachisu & M. Kato 2010, 2016, 2018b; I. Hachisu et al. 2020). We choose  $A_{\rm ff}$  for the 1.35  $M_{\odot}$  models to match that of the existing steady-state envelope model that has the closest chemical composition. The resultant light curves are very consistent with V1674 Her (see M. Kato et al. 2025, for more details).

For the 1.25  $M_{\odot}$  models, we have no corresponding steady-state envelope models with the same chemical composition. We determined  $A_{\rm ff}$  from an interpolation of steady-state envelope models in Tables 2 and 3 of I. Hachisu & M. Kato (2025a).

Figure 1 shows our theoretical light curves. Panel (a) shows three 1.35  $M_{\odot}$  WD models. Among them, the

<sup>&</sup>lt;sup>a</sup> Our control parameters in our model calculations are WD mass  $M_{\rm WD}$ , mass accretion rate  $\dot{M}_{\rm acc}$ , and carbon enhancement  $C_{\rm mix}$ . The other quantities are the results of our evolution calculations.



days since outburst

10

15

Figure 1. Theoretical model light curves for novae. (a) Our 1.35  $M_{\odot}$  WD model with mass-accretion rates of  $\dot{M}_{\rm acc}=1\times 10^{-11}~M_{\odot}~{\rm yr}^{-1}$  (cyan-blue line),  $5\times 10^{-10}~M_{\odot}~{\rm yr}^{-1}$  (red line), and  $5\times 10^{-9}~M_{\odot}~{\rm yr}^{-1}$  (black line). The origin of time (t=0) is set at the onset of thermonuclear runaway. The black dotted line indicates the sequence of steady-state wind solutions (M. Kato & I. Hachisu 1994) for a 1.35  $M_{\odot}$  WD with the envelope chemical composition of X=0.55, Y=0.3, Z=0.02,  $X_{\rm C}=0.03$  and  $X_{\rm O}=0.1$ . The radius at the bottom of the envelope (i.e., nuclear burning region) is assumed to be  $\log R/R_{\odot}=-2.48$ , which is taken from model M135ac5E-10. (b) Same as panel (a), but we added 1.25  $M_{\odot}$  WD models. The same color indicates the same accretion rate as that in panel (a). Orange line:  $\dot{M}_{\rm acc}=5\times 10^{-11}~M_{\odot}~{\rm yr}^{-1}$ . Gray line:  $1\times 10^{-10}~M_{\odot}~{\rm yr}^{-1}$ . Blue line:  $1\times 10^{-9}~M_{\odot}~{\rm yr}^{-1}$ .

lowest mass-accretion rate model of M135ac1E-11 shows the brightest peak. This model has the largest ignition mass among the three models (Table 1) so that the WD photosphere extends to the largest size among the three models. The wind mass-loss rate  $-\dot{M}_{\rm wind}^{\rm mas}$  is larger for a larger extended WD photosphere (M. Kato et al. 2025). The luminosity of free-free emission strongly depends on the wind mass-loss rate (see Equation (1)), so that it attains the brighter optical maximum. The highest mass-accretion rate model M135ac5E-9 shows a slower rise toward the optical maximum because the

ignition mass is smaller and this results in a lower maximum temperature  $T^{\rm max}$  at the nuclear burning region and a lower maximum nuclear burning rate  $L^{\rm max}_{\rm nuc}$  (see, e.g., M. Kato et al. 2024, for more details).

After day 4, the three model light curves converge into one. The dotted black line indicates the light curve for the sequence of steady-state envelope solutions which we call the steady state (light curve) model (I. Hachisu & M. Kato 2006). This indicates that the envelope structure settled down to a thermal equilibrium which is independent of the initial condition.

Figure 1(b) shows five 1.25  $M_{\odot}$  WD models (solid lines) in addition to the 1.35  $M_{\odot}$  WD models (dotted lines). The peak magnitudes of the 1.25  $M_{\odot}$  WD models are systematically higher than the 1.35  $M_{\odot}$  models because the ignition masses are larger and then the wind mass loss rate reaches a larger value. This tendency has been reported in Figure 6 of I. Hachisu et al. (2020): for  $M_{\rm WD} \gtrsim 1.1~M_{\odot}$ , the peak magnitude is fainter in a more massive WD with the same mass-accretion rate.

The five light curve models do not converge in this figure, but if we shift these models in the horizontal direction all the lines converge into one as shown later in Figure 2a.

# 3. COMPARISON OF MODEL LIGHT CURVES WITH FOUR NOVAE

In this section, we compare our theoretical light curves with the four classical novae listed in Table 2 whose optical peak are clearly observed including before and after the peak. These novae have been analyzed by comparing with steady state sequence models as well as by the timestretching method (e.g., I. Hachisu & M. Kato 2018b). Their WD masses and distance moduli in the V band  $\mu_V \equiv (m-M)_V$  are well constrained. In the present paper, we concentrate on the first few tens of days from the outburst to avoid secondary effects such as nebular emission lines, dust formation, and contributions from the optically-thin shocked shell. These effects occur outside the WD photosphere and contribute later to the light curves as analyzed in the papers listed in Table 2. We will summarize the effects of shock formation in Section 4.2.

#### 3.1. KT Eri 2009

KT Eri is a classical nova, discovered on UT 2009 November 25 (JD 2,455,160.5) at V=8.1 by K. Itagaki (Yamaoka et al. 2009). The orbital period is obtained to be  $P_{\rm orb}=2.6$  days (B. E. Schaefer et al. 2022), which is exceptionally long for classical novae.

тавіе	2.	Summary	OI	iour	novae

Object Outburst		$(m-M)_V$	E(B-V)	d	$M_{ m WD}$	$_{\text{reference}}a$
	year			(kpc)	$(M_{\odot})$	
V597 Pup	2007	$17.0 \pm 0.2$	0.3	$16 \pm 2$	$1.2 \pm 0.05$	1
KT Eri	2009	$13.4 \pm 0.2$	0.08	$4.2 \pm 0.4$	$1.3 \pm 0.02$	2
V339 Del	2013	$12.2 \pm 0.2$	0.18	$2.1\pm0.2$	$1.25\pm0.05$	3
SMCN 2016-10a	2016	$16.8 \pm 0.2$	0.08	$20.5\pm2$	$1.29 \pm 0.05$	4

 $<sup>^</sup>a$ 1: I. Hachisu & M. Kato (2010), 2: I. Hachisu et al. (2025), 3: I. Hachisu et al. (2024), 4: I. Hachisu & M. Kato (2018b)

Figure 2 shows the prediscovery light curve constructed by R. Hounsell et al. (2010) based on the data of the Solar Mass Ejection Imager (SMEI, R. Hounsell et al. 2010), which cover 3 magnitude rapid rise toward maximum followed by a much slower decay. The dense optical data around the optical peak enable us to accurately compare them with our theoretical light curves. In this figure we adopt the distance modulus in the V band of  $\mu_V \equiv (m-M)_V = 13.4$  after I. Hachisu et al. (2025) who obtained  $(m-M)_V = 13.4 \pm 0.2$  with the Gaia distance  $d = 4.2 \pm 0.4$  kpc (C. A. L. Bailer-Jones et al. 2021) and the reddening of  $E(B-V) = 0.08 \pm 0.02$  (G. M. Green et al. 2019).

Figure 2 also shows our model light curves. Figure 2(a) depicts the 1.25  $M_{\odot}$  WDs with five different mass accretion rates. Among them, the model with the mass accretion rate of  $\dot{M}_{\rm acc} = 5 \times 10^{-9}~M_{\odot}~{\rm yr}^{-1}$  shows a good agreement with the KT Eri light curve. In the later phase of t > 13 days, the light curve data becomes slightly fainter than our theoretical models, which suggests that a WD mass is possibly more massive than  $1.25~M_{\odot}$ .

Figure 2(b) shows our model light curves of a 1.35  $M_{\odot}$  WD. The cyan-blue circles are plotted for the same distance modulus of  $(m-M)_V=13.4$  as in panel (a). We choose its rising phase of KT Eri to match the red line (t=0) is the onset of thermonuclear runaway). In the rising phase the increasing rate is between the red line and black line, which is consistent with the peak magnitude, i.e., slightly fainter than the red line but brighter than the black line. After the peak, KT Eri (cyan-blue circles) shows a slower decline than these lines and much brighter than the  $1.35~M_{\odot}$  models after day 3.

We thus conclude that the  $1.35~M_{\odot}$  WD models do not correctly reproduce the KT Eri light curve. The slower decline of the cyan-blue circles in the post-maximum phase suggests that the WD mass is less massive than  $1.35~M_{\odot}$ , that is, the more massive the WD mass is, the faster/steeper the decay/slope of V light curve is (e.g., I. Hachisu & M. Kato 2006).

I. Hachisu et al. (2025) analyzed the KT Eri light curve over the full timespan of the outburst, i.e., from its optical peak until the end of the supersoft X-ray phase. Their light curve model is based on the steady-state sequence and included the contributions of an irradiated accretion disk and companion star which are effective in a later phase. They obtained the WD mass to be  $1.3 \pm 0.02~M_{\odot}$ , the mean mass accretion rate of  $\dot{M}_{\rm acc} \sim 1 \times 10^{-9}~M_{\odot}~{\rm yr}^{-1}$  in quiescent phase and the recurrence time to be  $t_{\rm rec} \sim 3000~{\rm yr}$ . The present light curve fitting is restricted to around the peak but includes the pre-maximum phase which is not analyzed in I. Hachisu et al. (2025). In spite of such differences, our light curve fitting in Figure 2 is consistent with their mass estimate.

KT Eri was once suggested to be a recurrent nova of the recurrence time  $t_{\rm rec} \sim 40$ –50 yr (e.g., B. E. Schaefer et al. 2022), but our results ( $t_{\rm rec} = 520$  yr for M125ac5E-9 in Table 1) clearly contradict the possibility of a recurrent nova ( $t_{\rm rec} \lesssim 100$  yr).

Also a good agreement with the KT Eri light curve confirms that our formulation of free-free emission model light curve, Equation (1), is reasonable.

# 3.2. V339 Del 2013

The classical nova V339 Del was discovered by Itagaki at 6.8 mag on UT 2013 August 14.584 (=JD 2,456,519.084, S. Nakano & N. N. Samus 2013). Immediately after the discovery, it was well observed in multiwavelength bands, especially in photometry, because of its brightness (a naked-eye nova;  $V \sim 4.4$  at peak). This is the first nova in which <sup>7</sup>Be lines are detected (A. Tajitsu et al. 2015): The first definit observational evidence of a thermonuclear runaway.

GeV gamma-rays were detected with the Fermi/LAT, first on JD 2,456,523 at the epoch depicted by the downward arrow in Figure 3(a) (M. Ackermann et al. 2014), and up to JD 2,456,547. The gamma-ray emission is closely related with a strong shock (L. Chomiuk et al. 2021, for a recent review). I. Hachisu et al. (2024) ana-

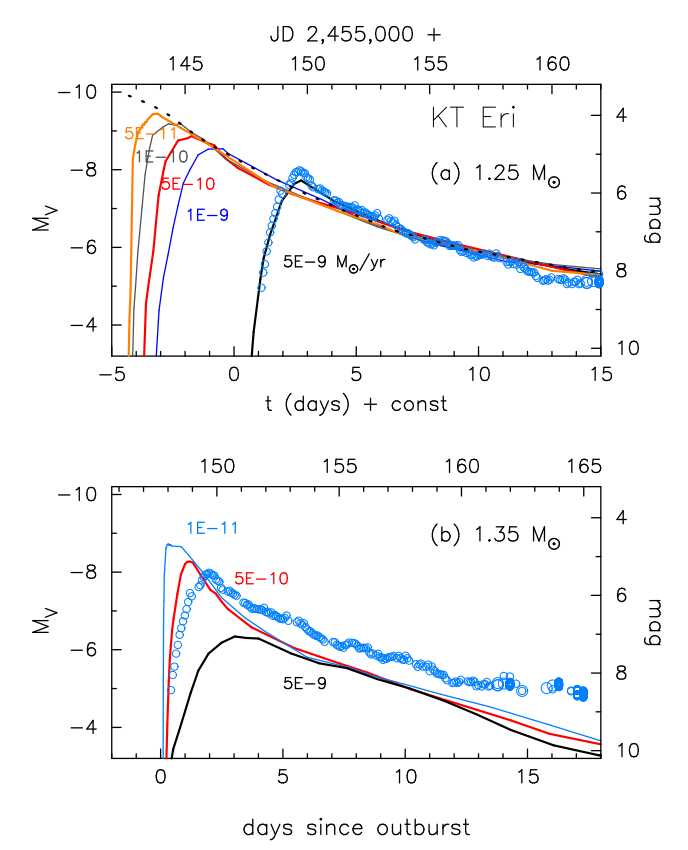
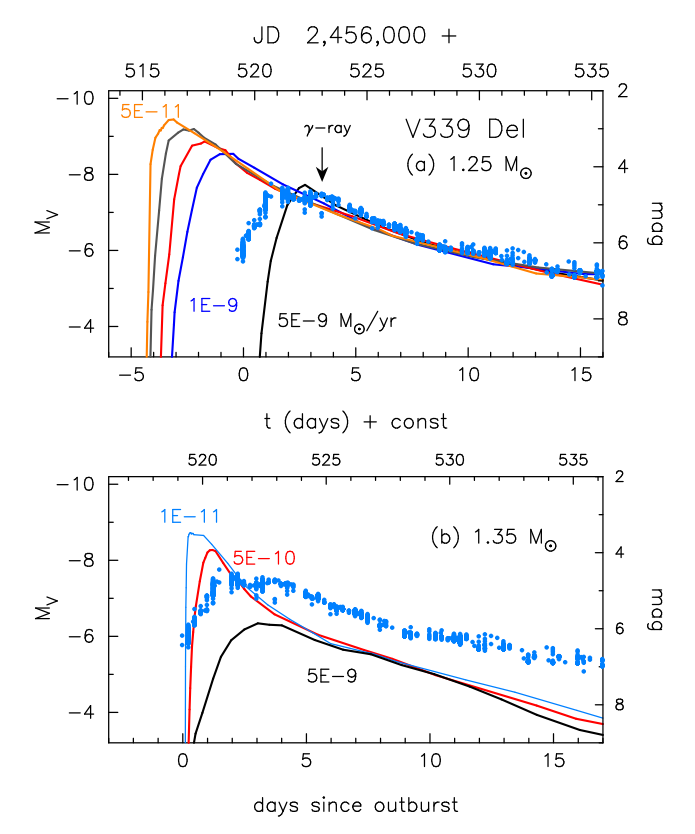


Figure 2. Comparison between the KT Eri V/SMEI light curves and our theoretical model light curves. The cyan-blue circles denote the KT Eri data for the distance modulus in the V band  $\mu_V \equiv (m-M)_V = 13.4$  as listed in Table 2. All the KT Eri data are the same as those in I. Hachisu et al. (2025), i.e., SMEI (before JD 2455162), and VSOLJ and AAVSO (after JD 2455151). (a) Each 1.25  $M_{\odot}$  WD model is shifted horizontally to fit the post-maximum phase with that of KT Eri. Thus, their outburst day is not just at t=0 but shifted by  $\Delta t$ . KT Eri is well fitted to the line of  $\dot{M}_{\rm acc} = 5 \times 10^{-9} \, M_{\odot} \, {\rm yr}^{-1}$ . The sequence of steady-state envelope solutions (dotted black line) is added for our 1.25  $M_{\odot}$  WD with the envelope chemical composition of X = 0.6,  $Y = 0.25, Z = 0.02, \text{ and } Z_{\text{CNO}} = 0.13.$  (b) Our 1.35  $M_{\odot}$ WD model light curves are depicted instead of the 1.25  $M_{\odot}$ WD models. The onset of thermonuclear runaway is at t = 0for all models.

lyzed multiwavelength light curve in detail including V, y,  $K_s$  of U. Munari et al. (2015), M.A. Burlak et al. (2015), SMARTS (F. M. Walter et al. 2012), and their own data, and X-ray light curves (Swift: P. A. Evans et al. 2009), and concluded that an optically thin dust-shell forms behind the shock. The epoch of dust formation, JD 2,456,553, is out of the range in Figure 3. Our nova evolution model does not include gamma-ray emission nor dust formation. However, the shock is formed far outside of the WD photopshere which does not affect our free-free emission light curve



**Figure 3.** Comparison between the V339 Del V and y light curves and our model light curves. The V339 Del V/y data (cyan-blue dots) are all taken from Figure 1 of I. Hachisu et al. (2024). Here, we assume  $(m-M)_V=12.2$  for V339 Del. (a) Fitting with the 1.25  $M_{\odot}$  WD models. The model light curve is shifted horizontally in the same way as in Figure 2. (b) Fitting with the 1.35  $M_{\odot}$  WD models. Three light curves are set at t=0.

around its peak. Gamma-ray emission and shock formation will be discribed in Discussion (Section 4.2).

I. Hachisu et al. (2024) analyzed multiwavelength light curve of V339 Del and obtained  $M_{\rm WD}=1.25\pm0.05~M_{\odot},~(m-M)_V=12.2\pm0.2,$  and  $d=2.1\pm0.2$  kpc for E(B-V)=0.18. Figure 3(a) shows y and V light curves assuming  $(m-M)_V=12.2$  together with our  $1.25~M_{\odot}$  WD models. These model light curves are shifted in the horizontal direction to match the decay phase of each model. Among the five  $\dot{M}_{\rm acc}$  models, the largest mass-accretion rate of  $\dot{M}_{\rm acc}=5\times10^{-9}~M_{\odot}~{\rm yr}^{-1}$  is reasonably fitted with the V339 Del light curve. The slight difference in the epoch of the rising phase indicates that the true mass-accretion rate is slightly smaller than  $5\times10^{-9}~M_{\odot}~{\rm yr}^{-1}$ , say,  $\dot{M}_{\rm acc}\sim3\times10^{-9}~M_{\odot}~{\rm yr}^{-1}$ .

Figure 3(b) shows the comparison between our 1.35  $M_{\odot}$  WD models and the V339 Del light curve. The cyan-blue data are the same as those in Figure 3(a). None of the 1.35  $M_{\odot}$  WD models can be fitted with the V339 Del light curve. The decline slope roughly agrees,

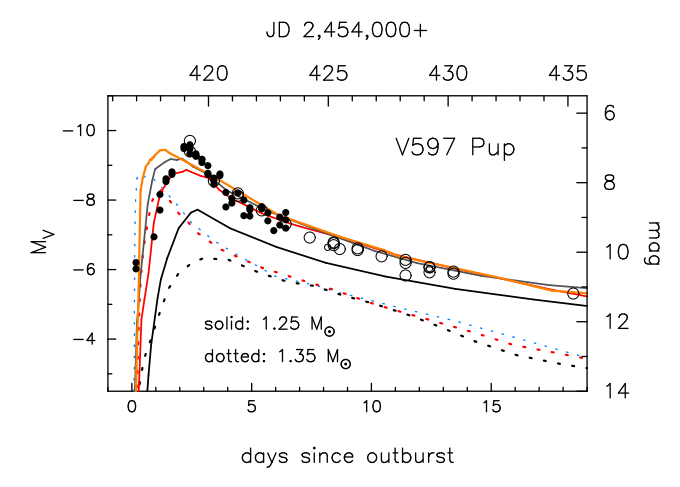


Figure 4. Comparison between the V light curve of the classical nova V597 Pup and our model light curves for  $(m-M)_V=17.0$ . The optical data are the same as those in I. Hachisu & M. Kato (2010). Filled circle: SMEI (R. Hounsell et al. 2010). Small open circle: AAVSO. Large open circle: VSOLJ. The solid lines are the model light curves for the 1.25  $M_{\odot}$  WD and the dotted lines are for the 1.35  $M_{\odot}$  WD models. The mass accretion rate of each model is the same as that of the same color model in Figure 1, in which model M125ac1E-9 is omitted to simplify the figure.

but slightly slower than the theoretical lines. This indicates that the WD mass is less massive than 1.35  $M_{\odot}$ .

The good agreement with the 1.25  $M_{\odot}$  WD model is consistent with the estimates of  $1.25\pm0.05~M_{\odot}$  of I. Hachisu et al. (2024) obtained from fitting with the post-maximum phase of V/y light curves. Their model light curves are based on the sequence of steady-state envelope solutions as introduced in Section 2.2 and Figure 1, but including the effects of an optically-thin shocked shell.

# 3.3. V597 Pup 2007#1

V597 Pup was discovered by Pereira on 2007 November 14.23 UT (JD 2454418.73) at mag about 7.0 (A.J.S. Pereira et al. 2007). The optical data are obtained with SMEI before the optical maximum followed by VSOLJ and AAVSO data. A bright supersoft X-ray phase was reported by J.-U. Ness et al. (2008c). The binary orbital period is 0.1112 day (2.6687 hr) by B. Warner & P.A. Woudt (2009)

I. Hachisu & M. Kato (2010) analyzed the optical and supersoft X-ray light curves of V597 Pup and estimated the WD mass to be  $1.2 \pm 0.05~M_{\odot}$ . They also determined  $(m-M)_V=17.0 \pm 0.2$  and the distance to V597 Pup,  $d=16 \pm 2$  kpc, for  $A_V=3.1E(B-V)=3.1 \times 0.3=0.93$  (J.-U. Ness et al. 2008c).

Figure 4 depicts the observed light curve of V597 Pup with  $(m-M)_V=17.0$ . The 1.25  $M_{\odot}$  mod-

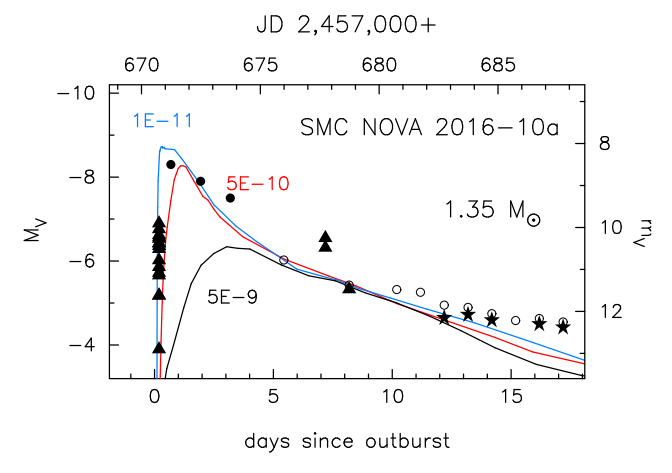


**Figure 5.** Comparison between the V light curve of the classical nova SMC Nova 2016-10a and our model light curves of the 1.35  $M_{\odot}$  WD models for  $(m-M)_V=16.8$ . The different symbols indicate different sources; Filled triangle: ATel No.9684 (F. Jablonski & A. Oliveira 2016), filled circle: ATel No.9631 (V. Lipunov et al. 2016), open circle: U. Munari et al. (2017), and filled stars: SMARTS (F. M. Walter et al. 2012). The reasonable fits by  $(m-M)_V=16.8$  indicate that SMC Nova 2016-10a is not a member of the SMC  $((m-M)_V=19.0, \text{ E. Aydi et al. 2017})$ , but a foreground Galactic nova.

els show better fits than the 1.35  $M_{\odot}$  models (dotted lines) that are all fainter than the observed brightness. Among the  $\dot{M}_{\rm acc}$  models of the 1.25  $M_{\odot}$  WD, the  $\dot{M}_{\rm acc}=5\times10^{-10}~M_{\odot}~{\rm yr}^{-1}$  model (red line) shows the closest fit.

The result is consistent with the WD mass estimate of  $1.2 \pm 0.05~M_{\odot}$  and with the distance modulus in the V band of  $(m-M)_V=17.0 \pm 0.2$  obtained by I. Hachisu & M. Kato (2010).

#### 3.4. SMCN 2016-10a

The classical nova SMCN 2016-10a appeared in the direction of  $(l,b)=(301^{\circ}.6362,-42^{\circ}.3037)$  toward the outskirt of the SMC. Thus, U. Munari et al. (2017) and E. Aydi et al. (2017) assumed that this object belongs to the SMC. On the other hand, I. Hachisu & M. Kato (2018b) obtained  $(m-M)_{V}=16.8$  and E(B-V)=0.08 using the color-magnitude  $(B-V)_{0}$ - $M_{V}$  diagram and time-stretching method for nova light curves (see Figure 36(c) of I. Hachisu & M. Kato 2018b). Then, the distance is d=20.5 kpc. They concluded that the classical nova SMCN 2016-10a is a foreground Galactic object. No orbital periods have ever been reported.

Here, we adopt  $(m-M)_V=16.8$  and plot our model light curves as well as the SMCN 2016-10a observation in Figure 5. The observational data are roughly consistent with the 1.35  $M_{\odot}$  WD model with the mass accretion rate of  $\dot{M}_{\rm acc}=5\times10^{-10}~M_{\odot}~\rm yr^{-1}$ . This confirms

that the distance d=20.5 kpc is reasonable and SMCN 2016-10a is not a member of the SMC, but a foreground Galactic object.

I. Hachisu & M. Kato (2018b) also analyzed light curves of V,  $I_C$ , and supersoft X-ray light curves and suggested that the WD mass is about 1.29  $M_{\odot}$ .

The light curve of SMCN 2016-10a is broadly consistent with the 1.35  $M_{\odot}$  with the mass-accretion rate of  $\dot{M}_{\rm acc}=1\times 10^{-11}~M_{\odot}~{\rm yr}^{-1}$  or  $\dot{M}_{\rm acc}=5\times 10^{-10}~M_{\odot}~{\rm yr}^{-1}$ . It should be noted that our model in Figure 5 is calculated with the solar heavy elements composition of Z=0.02 besides the extra carbon enrichment of  $X_C=0.1$ . Considering its location, far from the Galactic plane at z=-13.75 kpc, this nova is possibly a population II star ( $Z\leq 0.004$ ). If we take into account the tendency that a lower metallicity Z nova shows a slower decline (M. Kato et al. 2013), the WD mass of SMCN 2016-10a could be more massive than  $1.35~M_{\odot}$ .

# 4. DISCUSSION

# 4.1. Emission from the WD photosphere

In the present work, we have neglected the emission from the WD photosphere in calculating our theoretical V light curves.

I. Hachisu & M. Kato (2015) analyzed 11 slow/fast novae and clarified that the free-free emission from the optically thin ejecta just outside of the WD photophsere always dominates the WD photospheric emission (see their Figures 28 and 29), where they assumed blackbody approximation for the WD photospheric emission. I. Hachisu & M. Kato (2025b) clearly showed that the photospheric blackbody emission is rather small in the very fast nova V1674 Her (see their Figure 6). In fast novae, the flux of free-free emission substantially exceeds the flux of photospheric blackbody emission becasue their wind mass loss rates are large. In V1674 Her, V1500 Cyg, GK Per, and V603 Aql, the luminosity of the free-free emission is one order of magnitude larger ( $\sim$ 2.5 mag brighter) than that of the photospheric blackbody emission (I. Hachisu & M. Kato 2015, 2025b).

Figure 6 shows the light curves of the blackbody emission for all of our theoretical models. They are much fainter than the free-free luminosities. Thus, our assumption that we do not include the WD photospheric emission is appropriate.

#### 4.2. Shock Formation and Gamma-Ray Emission

GeV-gamma rays and hard X-rays have been often observed in nova outbursts, which are considered to originate from a strong shock between shells ejected with different velocities (e.g., K. Mukai & M. Ishida

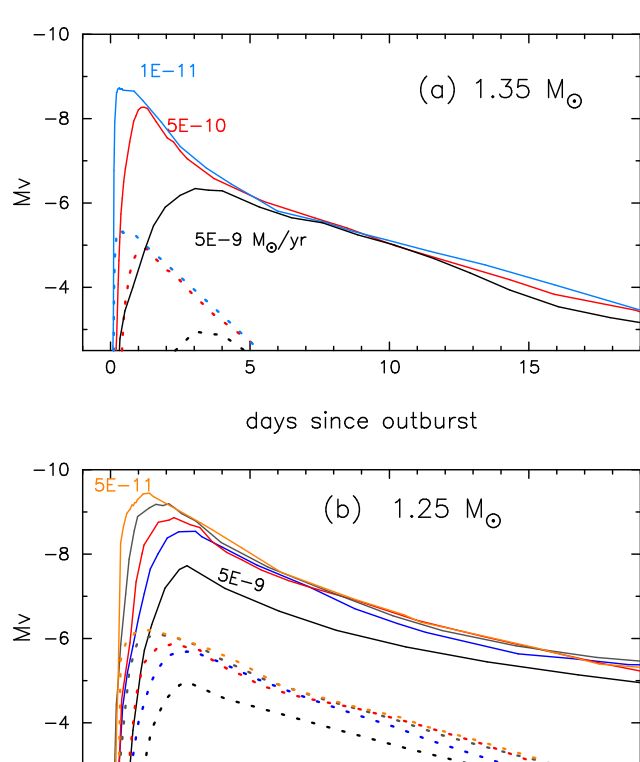


Figure 6. Comparison of V light curves between the freefree emission from the nova winds and the blackbody emission of the WD photosphere for each model. The models denoted by the thick lines are the same as in Figure 1. The dotted lines denote the V light curves for blackbody emission of the WD photosphere corresponding to the model with the same color.

10

days since outburst

15

0

2001; A. A. Abdo et al. 2010; M. Ackermann et al. 2014; C. C. Cheung et al. 2016; L. Chomiuk et al. 2014; T. Finzell et al. 2018; A. C. Gordon et al. 2021; P. Martin et al. 2018; B. D. Metzger et al. 2015; T. Nelson et al. 2012a; K. V. Sokolovsky et al. 2022). If the inner shell (later ejected) has a larger velocity than that of the outer shell (earlier ejected), the inner one can catch up with the outer one and forms a shock wave (e.g., K. Mukai & J. L. Sokoloski 2019; E. Aydi et al. 2020a,b). The assumption of multiple shell ejection is the key of this idea.

From the theoretical point of view, however, many numerical nova outburst calculations have been presented from the early thermonuclear runaway to the extended phase of nova outbursts (e.g., D. Prialnik & A. Kovetz 1992, 1995; N. Epelstain et al. 2007; Starrfield et al. 2009; P.A. Denissenkov et al. 2013; H.-L. Chen et al. 2019; M. Kato et al. 2022a,b), which show that mass

ejection is continuous, no multiple mass ejection occurs, therefore, no shock arises at the thermonuclear runaway.

I. Hachisu & M. Kato (2022) presented a shock formation mechanism based on M. Kato et al. (2022a)'s fully self-consistent nova explosion model. A strong reverse shock inevitably arises far outside of the WD photosphere after the optical peak because the later ejected matter has a larger expansion velocity that catches up the former ejected matter (see, e.g., Figure 1 of I. Hachisu & M. Kato 2022). I. Hachisu & M. Kato (2023) clarified that the shock devides expanding ejecta into three regions with different velocities, which naturally explains multiple velocity emission/absorption line systems (D. B. McLaughlin 1942; M. Friedjung This shock formation mechanism reasonably explains gamma-ray emission and hard X-ray detection/nondetection in classical novae (e.g., YZ Ret, V339) Del, and V392 Per in I. Hachisu & M. Kato 2023; I. Hachisu et al. 2024; I. Hachisu & M. Kato respectively).

Among the four novae studied in this paper, V339 Del is a gamma-ray nova. I. Hachisu et al. (2024) presented multiwavelength light curve model. The overall V and y light curves are explained by free-free emission from the ejcta just outside of the WD photophsere. The shocked shell is formed far outside the WD photopshere and its luminosity is one order of magnitude smaller than the free-free emission luminosity in the first 20 days (see Fig. 8(a) of I. Hachisu et al. 2024). They also explained the gamma-ray light curve from the optically thin shoked matter.

As the shocked shell is optically thin and its brightness is much smaller than the free-free emission, i.e., Equation (1), the light curve around the peak is not affectd by the presence/non-presence of the shocked shell. We thus assumed that our optical light curves can be applied to various novae independently of gamma-ray detection. We reasonably reproduced the light curves of KT Eri, V339 Del, V597 Pup, and SMC N 2016-10a only by our free-free emission models. This strongly supports that free-free emission dominates the nova luminosities if the shocked shell is optically thin.

# 4.3. Spherical Symmetry

We have assumed spherical symmetry in our nova outburst calculation. It is well known that some novae show asphericity of the ejecta (see, e.g., R. A. Downes & H. W. Duerbeck 2000, for old nova shells). As these images were taken much later than the optical peak, they are not the direct evidence of aspherical expansion at the epoch of optical peak.

It has been discussed that the sphericity (or elongation) of a nova shell depends on its (nova) speed class. The faster the nova speed class is, the more spherical the shell is (e.g., R. A. Downes & H. W. Duerbeck 2000). KT Eri ( $t_2 = 6.6$  days, R. Hounsell et al. 2010), V339 Del ( $t_2 = 10 \text{ days}$ , D. Chochol et al. 2014), V597 Pup ( $t_2 = 2.5 \text{ days}$ , S. Naik et al. 2009), and SMC N 2016-10a ( $t_2 = 4.0$  days, E. Aydi et al. 2018) belong to the very fast novae class ( $t_2 \leq 10$  days, C. Payne-Gaposchkin 1957) and its shell is probably close to spherical. Therefore, our assumption of spherical symmetry does not so largely depart from the true shell. This can be understood by the fact that a faster speed class of novae have larger expansion velocities and therefore their ejecta have less interaction times with the orbital motion of a companion star.

Before the WD photosphere reaches the companion star, its photospheric radius is as small as  $\lesssim 0.1~R_{\odot}$  and therefore is observed as an X-ray flash (O. König et al. 2022; M. Kato et al. 2022b). Such a case was seen in YZ Ret 2020, in which an X-ray flash is first detected. The X-ray luminosity during the flash phase, calculated from the observed blackbody temerature assuming spherical photosphere, is very consistent with the Eddington luminosity of a 1.35  $M_{\odot}$  WD (O. König et al. 2022; M. Kato et al. 2022b). This consistency supports that the WD photosphere is almost spherical and its shape does not much deviate from a sphere. In other words, this X-ray flash observation is the first direct indication of spherically symmetric expansion of the photopsere before the optical peak.

After the WD photosphere engulfs the companion star, free-free emission from the nova wind dominates the V luminosity. For one of the fastest class of novae, V1674 Her 2021 ( $t_2 = 0.9$  days, G. R. Habtie et al. 2024), I. Hachisu & M. Kato (2025b) showed that their free-free emission model V light curve calculated with Equation (1) for a 1.35  $M_{\odot}$  WD with  $\dot{M}_{\rm acc} = 1 \times$  $10^{-11} M_{\odot} \text{ yr}^{-1}$  almost perfectly reproduced the observed g band light curve in the rising phase from g = 15to 7 mag (see Figure 6 of I. Hachisu & M. Kato 2025b). This also confirms that the WD ejecta is almost spherically symmetric. In this case, the rising time from q=15to 7 mag is only 0.2 days, which is close to the orbital period of 0.153 days (J. Patterson et al. 2022). There seems to be almost no time to interact with the orbital motion.

#### 4.4. Comparison with steady-state models

The dotted black line in Figure 1(a) shows the light curve constructed from a time-sequence of steady-state envelope solutions on a 1.35  $M_{\odot}$  WD with

uniform chemical composition (I. Hachisu & M. Kato 2006, 2025a). This dotted line agrees well with the post-maximum phase of all the three fully self-consistent nova models. This indicates that in the post-maximum phase thermonuclear runaway almost settled down and the nuclear energy generation rate becomes almost constant with time (see, e.g., Figure 2 in M. Kato et al. 2025).

Figure 2(a) shows the steady-state sequence model of the 1.25  $M_{\odot}$  with the chemical composition of X=0.6, Y=0.25,  $Z_{\rm CNO}=0.13$ , and Z=0.02 and the radius of the envelope to be  $\log R/R_{\odot}=-2.29$ . Our model light curve follows well the steady-state sequence model in the post-maximum phase.

To summarize, soon after the optical peak, a nova explosion evolution can be approximated by a sequence of steady-state solutions with decreasing envelope mass as already reported in a fully self-consistent nova explosion model on a 1.0  $M_{\odot}$  WD (M. Kato et al. 2022a).

M. Kato (1983) proposed an idea that nova explosions can be followed by a sequence of steady-state optically-thick wind solutions with the decreasing envelope mass because a nova envelope would settle down to a steady state shortly after a thermonuclear run-This optically thick nova away reaches maximum. wind theory was formulated by M. Kato & I. Hachisu (1994). Based on the steady-state envelope sequences, I. Hachisu & M. Kato (2006) calculated a number of free-free emission model nova light curves. Many novae have been analyzed with these free-free emission model nova light curves and their WD masses have been determined. The present work on the 1.25  $M_{\odot}$  and 1.35  $M_{\odot}$ WDs gives an additional theoretical support to these nova light curve analyses.

#### 5. CONCLUSION

Our results are summarized as follows:

1. We present theoretical light curves of classical novae for 1.25  $M_{\odot}$  and 1.35  $M_{\odot}$  WDs. Our numeri-

cal code is a Henyey-type evolution code combined with the optically thick winds. The optical V light curve is calculated for free-free emission. Our V light curves predict nova light curves, from a rising phase toward optical maximum and the early decay phase.

- 2. We have compared our light curves with those of the classical novae, KT Eri, V339 Del, V597 Pup, and SMC Nova 2016-10a whose WD masses and distance moduli in the V band are well constrained. Our models show excellent agreements with these novae. The WD masses of these novae are consistent with the results in Table 2, which are independently obtained from the entire decay phase of novae including the X-ray light curve fittings of their SSS phases.
- These good agreements with the V light curves support that the rising phase toward optical maximum is well approximated by our free-free emission model light curves.
- 4. We confirm that the time-sequence of steady-state envelope solutions with the decreasing envelope mass is a good approximation to nova outburst explosions on the 1.25  $M_{\odot}$  and 1.35  $M_{\odot}$  WDs in the post-maximum phase.

We thank the American Association of Variable Star Observers (AAVSO) for the archival data of KT Eri, V597 Pup and the Variable Star Observers League of Japan (VSOLJ) for V597 Pup. We are also grateful to the anonymous referee for useful comments regarding how to improve the manuscript.

# REFERENCES

Abdo, A. A., Ackermann, M., Ajello, M., et al. 2010, Science, 329, 817,

https://doi.org/10.1126/science.1192537

Ackermann, M., Ajello, M., Albert, A., et al. 2014, Science, 345, 554, https://doi.org/10.1126/science.1253947

Aydi, E., Page, K. L., Kuin, N. P. M., et al. 2017, MNRAS, 474, 2679, https://doi.org/10.1093/mnras/stx2678

Aydi, E., Page, K. L., Kuin, N. P. M., et al. 2018, MNRAS, 474, 2679, https://doi.org/10.1093/mnras/stx2678 Aydi, E., Chomiuk, L., Izzo, L., et al. 2020a, ApJ, 905, 62, https://doi.org/10.3847/1538-4357/abc3bb

Aydi, E., Sokolovsky, K. V., Chomiuk, L., et al. 2020b, Nature Astronomy, 4, 776,

Bailer-Jones, C.A.L., Rybizki, J., Fouesneau, M., Demleitner, M., & Andrae, R. 2021, AJ, 161, 147,

https://doi.org/10.3847/1538-3881/abd806

https://doi.org/10.1038/s41550-020-1070-y

- Buckley, D. A. H., & Tuohy, I.R. 1989, ApJ, 344, 376, https://doi.org/10.1086/167806
- Burlak, M. A., Esipov, V. F., Komissarova, G. V., et al. 2015, Baltic Astronomy, 24, 109, https://doi.org/10.1515/astro-2017-0209
- Chen, H.-L., Woods, T. E., Yungelson, L. R., et al. 2019, MNRAS, 490, 1678,

https://doi.org/10.1093/mnras/stz2644

- Cheung, C. C., Jean, P., Shore, S. N., et al., ApJ, 826, 142 https://doi.org/10.3847/0004-637X/826/2/142
- Chochol, D., Shugarov, S., Pribulla, T., Volkov, I. 2014, CoSka, 43, 330
- Chomiuk, L., Linford, J. D., Yang, J., et al. 2014, Nature, 514, 339, https://doi.org/10.1038/nature13773
- Chomiuk, L., Metzger, B. D., & Shen, K. J. 2021, Annual Review of Astronomy and Astrophysics, 59, 48, https://doi.org/10.1146/annurev-astro-112420-114502
- Denissenkov, P. A., Herwig, F., Bildsten, L., & Paxton, B. 2013, ApJ, 762, 8

 $\rm https://doi.org/10.1088/0004\text{-}637X/762/1/8$ 

- Downes, R. A., & Duerbeck, H. W. 2000, AJ, 120, 2007, https://doi.org/10.1086/301551
- Ennis, D., Becklin, E. E., Beckwith, S., et al. 1977, ApJ, 214, 478, https://doi.org/10.1086/155273
- Epelstain, N., Yaron, O., Kovetz, A., & Prialnik, D. 2007, MNRAS, 374, 1449,

https://doi.org/10.1111/j.1365-2966.2006.11254.x

Evans, P. A., Beardmore, A. P., Page, K. L., et al. 2009, MNRAS, 397, 1177,

https://doi.org/10.1111/j.1365-2966.2009.14913.x

- Finzell, T., Chomiuk, L., Metzger, B. D., et al. 2018, ApJ, 852, 108, https://doi.org/10.3847/1538-4357/aaa12a
- Friedjung, M. 1966, MNRAS, 132, 317, https://doi.org/10.1093/mnras/132.2.317

Friedjung, M. 1987, A&A, 180, 155

- Gallagher, J. S., & Ney, E. P. 1976, ApJ, 204, L35, https://doi.org/10.1086/182049
- Gehrz, R. D., Truran, J. W., Williams, R. E., & Starrfield, S. 1998, PASP, 110, 3, https://doi.org/10.1086/316107
- Gordon, A. C., Aydi, E., Page, K. L., et al. 2021, ApJ, 910, 134, https://doi.org/10.3847/1538-4357/abe547
- Green, G. M., Schlafly, E. F., Zucker, C., et al. 2019, ApJ, 887, 93 https://doi.org/10.3847/1538-4357/ab5362
- Habtie, G. R. Das, R., Pandey, R., Ashok, N.M., & Dubovsky, P.A. 2024, MNRAS, 527, 1405, https://doi.org/10.1093/mnras/stad3295
- Hachisu, I., & Kato, M. 2006, ApJS, 167, 59 https://doi.org/10.1086/508063
- Hachisu, I., & Kato, M. 2010, ApJ, 709, 680, https://doi.org/10.1088/0004-637X/709/2/680

- Hachisu, I., & Kato, M. 2015, ApJ, 798, 76, https://doi.org/10.1088/0004-637X/798/2/76
- Hachisu, I., & Kato, M. 2016, ApJ, 816, 26, https://doi.org/10.3847/0004-637X/816/1/26
- Hachisu, I., & Kato, M. 2018a, ApJ, 858, 108, https://doi.org/10.3847/1538-4357/aabee0
- Hachisu, I., & Kato, M. 2018b, ApJS, 237, 4, https://doi.org/10.3847/1538-4365/aac833
- Hachisu, I., & Kato, M. 2019a, ApJS, 241, 4, https://doi.org/10.3847/1538-4365/ab0202
- Hachisu, I., & Kato, M. 2019b, ApJS, 242, 18, https://doi.org/10.3847/1538-4365/ab1b43
- Hachisu, I., & Kato, M. 2021, ApJS, 253, 27, https://doi.org/10.3847/1538-4365/abd31e
- Hachisu, I., & Kato, M. 2022, ApJ, 939, 1 https://doi.org/10.3847/1538-4357/ac9475
- Hachisu, I., & Kato, M. 2023, ApJ, 953, 78, https://doi.org/10.3847/1538-4357/acdfd3
- Hachisu, I., & Kato, M. 2025a, ApJ, 984, 136, https://doi.org/10.3847/1538-4357/adc38a
- Hachisu, I., & Kato, M. 2025b, ApJ, 989, 153, https://doi.org/10.3847/1538-4357/adef0b
- Hachisu, I., Kato, M., & Matsumoto, K. 2024, ApJ, 965, 49, https://doi.org/10.3847/1538-4357/ad2a45
- $$\label{eq:hachisu} \begin{split} & \text{Hachisu, I., Kato, M., \& Walter, F. M. 2025, ApJ, 980, 142,} \\ & \text{https://doi.org/} & 10.3847/1538-4357/adae08 \end{split}$$
- Hachisu, I., Saio, H., Kato, M., Henze, M., & Shafter, A. W. 2020, ApJ, 902, 91,
  - https://doi.org/10.3847/1538-4357/abb5fa
- Henze, M., Darnley, M., Williams, S. C. et al. 2018, ApJ, 857, 68, https://doi.org/10.3847/1538-4357/aab6a6
- Henze, M., Ness, J.-U., Darnley, M., et al. 2015, A&A, 580, 46
- Henze, M., Pietsch, W., Haberl, F., Hernanz, M., Sala, G., Hatzidimitriou, D., Della Valle, M., Rau, A. et al. 2011, A&A, 533, A52,

https://doi.org/10.1051/0004-6361/201015887

- Hillman, Y., Prialnik, D., Kovetz, A., Shara, M. M., & Neill, J. D. 2014, MNRAS, 437, 1962 https://doi.org/10.1093/mnras/stt2027
- Hillman, Y., Prialnik, D., Kovetz, A., & Shara, M. M. 2016, ApJ, 819, 168
  - https://doi.org/10.3847/0004-637X/819/2/168
- Hounsell, R., Bode, M. F., Hick, P. P., et al. 2010, ApJ, 724, 480, https://doi.org/10.1088/0004-637X/724/1/480
- Iben, I. Jr. 1982, ApJ, 259, 244,

https://doi.org/10.1086/160164

Iglesias, C.A., & Rogers, F.J. 1993, ApJ, 412, 752, https://doi.org/10.1086/172958

- Iglesias, C. A., & Rogers, F. J. 1996, ApJ, 464, 943, https://doi.org/10.1086/177381
- Jablonski, F., & Oliveira, A. 2016, AT<br/>el, 9684,  $\boldsymbol{1}$
- Kato, M., 1983, PASJ, 35, 507
- Kato, M., & Hachisu, I., 1994, ApJ, 437, 802, https://doi.org/10.1086/175041
- Kato, M., Hachisu, I., Henze, M. 2013, ApJ, 779, 19 https://doi.org/10.1088/0004-637X/779/1/19
- Kato, M., Hachisu, I., & Saio, H. 2017a, PoS, GOLDEN 2017, 56 in Proceedings of the Palermo Workshop 2017 on "The Golden Age of Cataclysmic Variables and Related Objects IV", eds. F. Giovannelli et al. (Trieste: SISSA PoS), 315, 56, https://doi.org/10.22323/1.315.0056 (arXiv: 1711.01529) https://pos.sissa.it/315/056/pdf
- Kato, M., Hachisu, I., Saio, H. 2025, ApJ, 988,112 https://doi.org/10.3847/1538-4357/ade231
- Kato, M., Saio, H., & Hachisu, I. 2022a, PASJ, 74, 1005, https://doi.org/10.1093/pasj/psac051
- Kato, M., Saio, H, & Hachisu, I. 2022b, ApJL, 935, L15, https://doi.org/10.3847/2041-8213/ac85cl
- Kato, M., Saio, H, & Hachisu, I. 2022c, Research notes of the AAS, 6, 258,
  - https://doi.org/10.3847/2515-5172/aca8af
- Kato, M., Saio, H, & Hachisu, I. 2024, PASJ, 76, 666, https://doi.org/10.1093/pasj/pase038
- Kato, M., Saio, H., Hachisu, I., Nomoto, K. 2014, ApJ, 793, 136
- König, O., Wilms, J., Arcodia, R., et al. 2022, Nature, 605, 248, https://doi.org/10.1038/s41586-022-04635-y
- Krautter, J., Ögelman, H., Starrfield, S., Wichmann, R., & Pfeffermann, E. 1996, ApJ, 456, 788 https://doi.org/10.1086/176697
- Lico, R. et al. 2024 A&A, 692,A107 https://doi.org/10.1051/0004-6361/202451364
- Lipunov, V., Podesta, R., Levato, H., et al. 2016, ATel, 9631, 1
- Ma, X., Chen, X., Chen, H-l, Denissenkov, P.A., Han, Z. 2013, ApJL, 778 32,
  - https://doi.org/10.1088/2041-8205/778/2/L32
- Martin, P., Dubus, G., Jean, P., Tatischeff, V., & Dosne, C. 2018, A&A, 612, A38,
  - $\rm https://doi.org/10.1051/0004\text{-}6361/201731692$
- MacDonald, J. 1980, MNRAS, 191, 933, https://doi.org/10.1093/mnras/191.4.933
- McLaughlin, D. B. 1942, ApJ, 95, 428, https://doi.org/10.1086/144414
- Metzger, B. D., Finzell, T., Vurm, I., et al. 2015, MNRAS, 450, 2739, https://doi.org/10.1093/mnras/stv742
- Mukai, K., & Ishida, M. 2001, ApJ, 551, 1024, https://doi.org/10.1086/320220

- Mukai, K., & Sokoloski, J. L. 2019, Physics Today 72, 11, 38, https://doi.org/10.1063/PT.3.4341
- Munari, U., Maitan, A., Moretti, S., Tomaselli, S. 2015, NewA, 40, 28,
  - https://doi.org/10.1016/j.newast.2015.03.008
- Munari, U., Hambsch, F.-J., & Frigo, A. 2017, MNRAS, 469, 4341
- Naik, S., Banerjee, D. P. K., & Ashok, N. M. 2009, MNRAS, 394, 1551,
  - https://doi.org/10.1111/j.1365-2966.2009.14421.x
- Nakano, S., & Samus, N. N. 2013, IAUC, 9258, 1
- Nariai, K., Nomoto, K., & Sugimoto, D. 1980, PASJ, 32, 473
- Ness, J.-U., et al. 2008c, IAUC, 8911, 2
- Newsham, G., Starrfield, S., & Timmes, F.X. 2014, ASP conference Series, Vol.490, Stella Novae: Past and Future Decades,287
- Nelson, T., Donato, D., Mukai, K., Sokoloski, J., & Chomiuk, L. 2012a, ApJ, 748, 43,
- https://doi.org/10.1088/0004-637X/748/1/43
- Nomoto, K. 1982, ApJ, 253, 798, https://doi.org/10.1086/159682
- Özdörmez, A., Ege, E., Güver, T., & Ak, T. 2018, MNRAS, 476, 4162, https://doi.org/10.1093/mnras/sty432
- Page, K. L., Beardmore, A. P., Osborne, Jp, P., Munari, U., Ness, U.-U. et al. 2022, A&A, 514, 1557
- Patterson, J., Enenstein, J, de Miguel, E., et al. 2022, ApJL, 940, L56,
  - https://doi.org/10.3847/2041-8213/ac9ebe
- Payne-Gaposchkin, C. 1957, The galactic Novae (Amsterdam: North-Holland)
- Pereira, A., di Cicco, D., Vitorino, C., & Green, D. W. E. 1999, IAUC, 7323, 1
- Pereira, A. J. S., McGaha, J. E., Young, J., & Rhoades, H. 2007, IAUC, 8895, 1
- Prialnik, D., & Kovetz, A. 1992, ApJ, 385, 665, https://doi.org/10.1086/170972
- Prialnik, D., & Kovetz, A. 1995, ApJ, 445, 789, https://doi.org/10.1086/175741
- Ruggles, C. L. N. & Bath, G. T. 1979, A&A, 80, 97
- Shen, K. J, & Quataert, E. 2022, ApJ, 938, 31,
  - https://doi.org/10.3847/1538-4357/ac9136
- Schaefer, B.E., 2022a, MNRAS, 517, 3640, https://doi.org/10.1093/mnras/stac2089
- Schaefer, B. E., Walter, F. M., Hounsell, R., Hillman, Y. 2022, MNRAS, 517, 3864,
  - $\rm https://doi.org/10.1093/mnras/stac2923$
- Schaefer, B. E. 2022b, MNRAS, 517, 6150,
  - https://doi.org/10.1093/mnras/stac2900

- Schwarz, G. J., Shore, S. N., Starrfield, S., & Vanlandingham, K. M. 2007, ApJ, 657,453, https://doi.org/10.1086/5106611
- Schwarz, G. J., Ness, J.-U., Osborne, J. P., Page, K. L., Evans, P. A., et al. 2011, /apjs, 197, 31, https://doi.org/10.1088/0067-0049/197/2/31
- Seaton, M. J., Yan, Y., Mihalas, D., Pradhan, A., K., 1994, MNRAS, 266, 805, https://doi.org/10.1093/mnras/266.4.805
- Sion, E. M., Acierno, M.J., & Tomczyk, S. 1979, ApJ, 230, 832, https://doi.org/10.1086/157143
- Sokolovsky, K. V., Li, K.-L., Lopes de Oliveira, R., et al. 2022, MNRAS, 514, 2239,
  - https://doi.org/10.1093/mnras/stac1440
- Sokolovsky, K. V., Johnson, T.J., Buson, S., et al. 2023, MNRAS, 521,5453,
  - https://doi.org/10.1093/mnras/stad887
- Sparks, W. N., Starrfield, S., & Truran J. W. 1978, ApJ, 220, 1063, https://doi.org/10.1086/155992
- Starrfield, S., Iliadis, C., Hix, W. R., Timmes, F. X., & Sparks, W. M. 2009, ApJ, 692, 1532, https://doi.org/10.1088/0004-637X/692/2/1532
- Starrfield, S., Bose, M., Iliadis, C. et al. 2020, ApJ, 895, 70, https://doi.org/10.3847/1538-4357/ab8d23

- Tajitsu, A., Sadakane, K., Naito, H., Arai, A., Aoki, W. 2015, Nature, 518, 381, https://doi.org/10.1038/nature14161
- Vanlandingham, K. M., Starrfield, S., & Shore, S. N. 1997, MNRAS, 290, 87,
  - https://doi.org/10.1093/mnras/290.1.87
- Vanlandingham, K. M., Starrfield, S., Wagner, R. M., Shore, S. N., & Sonneborn, G. 1996, MNRAS, 282, 563 https://doi.org/10.1093/mnras/282.2.563
- Warner, B. 1995, Cataclysimic variable stars, Cambridge astrophysics series:28, (Cambridge University Press: New York
- Walter, F. M., Battisti, A., Towers, S. E., Bond, H. E., & Stringfellow, G. S. 2012, PASP, 124, 1057, https://doi.org/10.1086/668404
- Warner, B., & Woudt, P. A. 2009, MNRAS, 397, 979, https://doi.org/10.1111/j.1365-2966.2009.15006.x
- Wu, C., Wang, B., Liu, D., & Han, Z. 2017, A&A, 604, 31, https://doi.org/10.1051/0004-6361/201630099
- Yamaoka, H., Itagaki, K., Guido, E. 2009, IAUC, 9098, 1